

PET/PDT Theranostics: Synthesis and Biological Evaluation of a Peptide-Targeted Gallium Porphyrin

F. Bryden^a, H. Savoie^a, E.V. Rosca^b, R.W. Boyle^{a*}

The development of novel theranostic agents is an important step in the pathway towards personalised medicine, with the combination of diagnostic and therapeutic modalities into a single treatment agent naturally lending itself to the optimisation and personalisation of treatment. In pursuit of the goal of a molecular theranostic suitable for use as a PET radiotracer and a photosensitiser for PDT, a novel radiolabelled peptide-porphyrin conjugate targeting the $\alpha_6\beta_1$ -integrin has been developed. $^{69/71}\text{Ga}$ and ^{68}Ga labelling of an azide-functionalised porphyrin has been carried out in excellent yields, with subsequent bioconjugation to an alkyne-functionalised peptide demonstrated. $\alpha_6\beta_1$ -integrin expression of two cell lines has been evaluated by flow cytometry, and therapeutic potential of the conjugate demonstrated. Evaluation of the phototoxicity of the porphyrin-peptide theranostic conjugate in comparison to an untargeted control porphyrin *in vitro*, demonstrated significantly enhanced activity for a cell line with higher $\alpha_6\beta_1$ -integrin expression when compared with a cell line exhibiting lower $\alpha_6\beta_1$ -integrin expression.

Introduction

The goal of developing personalised medicine is an emerging trend within both clinical and scientific areas of research, and is of particular interest in the treatment of neoplastic conditions. Tumour heterogeneity in patient populations can be vast and can lead to significant differences in patient outcomes when using standardised treatments. It is unsurprising, that the development of novel theranostics is also a growing trend in research, with the combination of diagnostic and therapeutic modalities into a single agent naturally lending itself to the optimisation and personalisation of treatment. While the majority of work in the area of theranostics utilises nanoparticles either for conjugation, or encapsulation, of two or more distinct treatment and imaging agents (see Xie *et al* for a comprehensive review¹), progress has also been seen in the area of molecular theranostics, allowing the combination of therapeutic and diagnostic abilities without the need for synthesis of complex nanostructures.

Porphyrins naturally lend themselves to the area of molecular theranostics, with many examples in the literature of their separate use in both therapeutic and diagnostic capacities. The therapeutic abilities of porphyrins are undisputed; their favourable photophysical properties, and relative ease of both synthesis and functionalization, has led to their dominance in the field of photodynamic therapy; with their potent and selective cytotoxic action on tumour tissue being extensively documented^{2, 3}. In addition, while both endogenous and exogenous free-base porphyrins have cemented their position as field-leaders in the area of fluorescent imaging⁴, the utility of porphyrins as chelators for a host of metals suitable for imaging applications allows the use of these metallated porphyrins as positron emission tomography (PET), single-photon emission computed tomography (SPECT) or magnetic resonance imaging (MRI) agents.⁵

PET imaging is of particular interest for theranostic applications, offering functional imaging for the detection of metabolic changes in neoplastic tissues, rather than the mainly structural imaging offered by MRI. This provides good quality images while

minimising the need for invasive biopsies to determine tumour malignancy. While the clinically approved ^{18}F radiolabelled 2-fluorodeoxyglucose (FDG) is currently considered to be the “gold standard” of PET-imaging agents, uptake of FDG is an untargeted process, relying solely on the increased metabolism of the neoplastic tissue to promote tumour localisation. Development of alternative radiotracers which target tumour-associated receptors allows characterisation of cell biomarker expression and can give an indication of prognosis as well as allowing personalised planning of treatment. In particular, the radiolabelling of therapeutic agents such as photosensitisers also provides valuable information regarding the uptake and localisation of the molecule, as well as providing an indication of likely responses to PDT treatment.

The vast majority of porphyrin radiolabelling strategies in the literature have utilised the porphyrin as a chelating agent for radioisotopes such as Cu-64^{6-8} , Ga-68^{9-11} , and Nd-140^{12} (see Waghorn *et al.* for a comprehensive review of radiolabelled porphyrins¹³). However, chelation of paramagnetic isotopes quenches the therapeutic action of the porphyrin, requiring use of the unmetallated porphyrin as the treatment agent. This is a major limitation in utilising radioisotopes such as ^{64}Cu , since it necessitates the administration of therapeutic and diagnostic agents in separate doses, with an appropriate delay between these doses to allow clearance of the radiolabelled species. In addition, it has previously been demonstrated that alteration in tumour uptake can occur upon metallation of porphyrin photosensitisers^{14, 15}, limiting the usefulness of any imaging data generated in this way. As gallium (III) is diamagnetic, chelation of ^{68}Ga by the porphyrin photosensitiser can be utilised to produce a theranostic which maintains functionality as both a PDT and a PET agent.

Despite the potential utility of ^{68}Ga porphyrins as diagnostic agents, to date there have been few published examples of the development of these metallo-porphyrins as radiotracers for PET. ^{68}Ga radiolabelling of both exogenous¹¹, and targeted⁹ and untargeted¹⁰ endogenous porphyrins has been carried out in radiochemical yields (RCY) of between 22-73%, with the utility of these radiotracers as both PET^{10, 11} and fluorescent⁹ imaging agents demonstrated. However, to date no examples of gallium-labelled porphyrins have undergone biological evaluation as therapeutic agents, and no examples of ^{68}Ga radiolabelling of exogenous, water-soluble porphyrins have been published.

It was therefore envisaged that the development of novel targeted theranostic agents could be achieved through the combination of the demonstrated radiolabelling potential of porphyrins with our current interest in the mild bio-orthogonal conjugation of porphyrin photosensitisers to targeting moieties¹⁶⁻¹⁸ through use of the Copper-Catalysed Azide-Alkyne Cycloaddition (CuAAC) reaction. This reaction is mild and generally high yielding^{19, 20} and has been shown to be highly compatible with both porphyrin bioconjugation and radiochemistry, being largely insensitive to steric hindrance and operating well in aqueous conditions without the need for high temperatures or long reaction times.

Results and discussion

Evaluation of cell receptor expression

Conjugation of a targeting peptide to the radiolabelled porphyrin was selected as this strategy is highly compatible with short-lived radioisotopes; the small size of peptides allows accumulation in target tissue in a short time period, and rapid clearance from the bloodstream. Imaging of the cell-surface integrin receptors utilising PET has previously been demonstrated utilising both ^{68}Ga - and ^{18}F -^{21, 22} labelled peptides and has been shown to be particularly effective in the determination of both metastasis and angiogenesis associated with tumours.

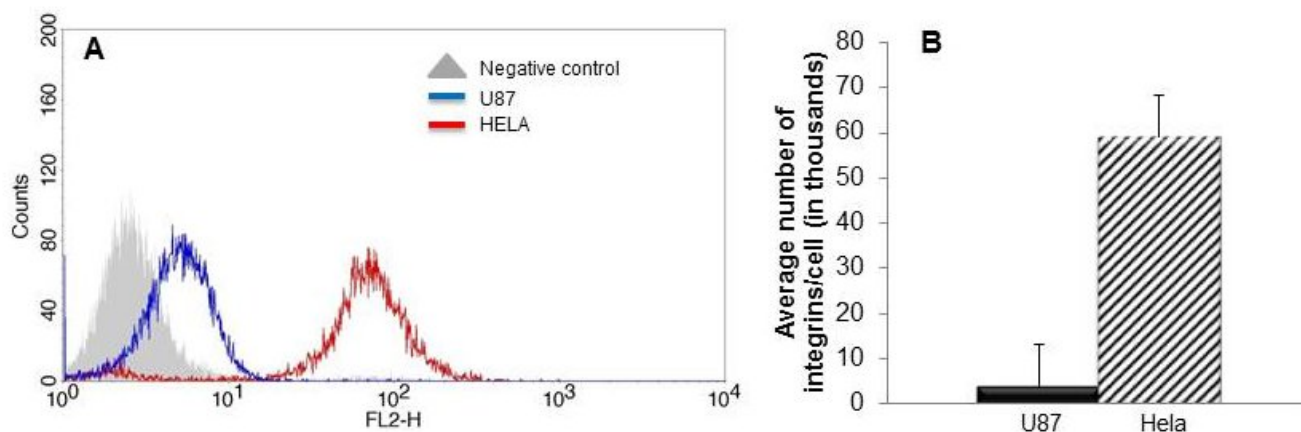
The dodecapeptide TWYKIAFQRNRK was first characterised in 1996 by Nakahara *et al.*²³, and exhibits a good affinity for the $\alpha_6\beta_1$ -integrin²⁴. While this integrin is involved in cellular migration and adhesion in normal tissue, it is also upregulated in multiple cancers, including breast carcinomas and glioblastomas, in which it is associated with the facilitation of tumorigenesis and promotion of metastasis.²⁵ Despite this, the use of this peptide in imaging applications is controversial, as its binding has in some cases demonstrated stimulation of the invadopodial activity of the integrin.²⁶ However, use in targeted theranostic conjugates would allow treatment immediately following imaging, limiting the deleterious effects of the integrin signalling activation.

In order to confirm retention of the $\alpha_6\beta_1$ -integrin targeting ability of the peptide following synthesis of the porphyrin-peptide theranostic, two cell lines exhibiting a differential in $\alpha_6\beta_1$ -integrin expression were required. However, due to the essential roles played by the $\alpha_6\beta_1$ -integrin in normal cells some basal expression is always present, and therefore knock out of integrin expression in order to generate a “negative” control cell line does not produce an accurate model of the *in vivo* environment. For this reason, we evaluated two cell lines to ascertain the differential in their natural integrin expression *via* relative fluorescent intensity. As

illustrated in panel A of figure 1, a large dynamic range of expression was observed, with the cell lines displaying natural integrin receptor quantities over two orders of magnitude.

In order to quantify how these levels of expression could be correlated to the number of receptors, fluorescently calibrated beads were used in order to provide quantification of the number of receptors on the cell surface (panel B of Figure 1). In particular, the U87 cell line was shown to have extremely low levels of integrin expression, while in contrast the HeLa cell line was found to be integrin high expressing.

Figure 1: Quantification of integrin expression on cell surface. Panel A depicts relative fluorescence intensity of cells measured by FACS; the grey histogram depicts the negative control which is similar between the different cells. Panel B depicts the quantification of the receptor number per cell accomplished with calibrated fluorescence beads. The error bars depict standard deviation.

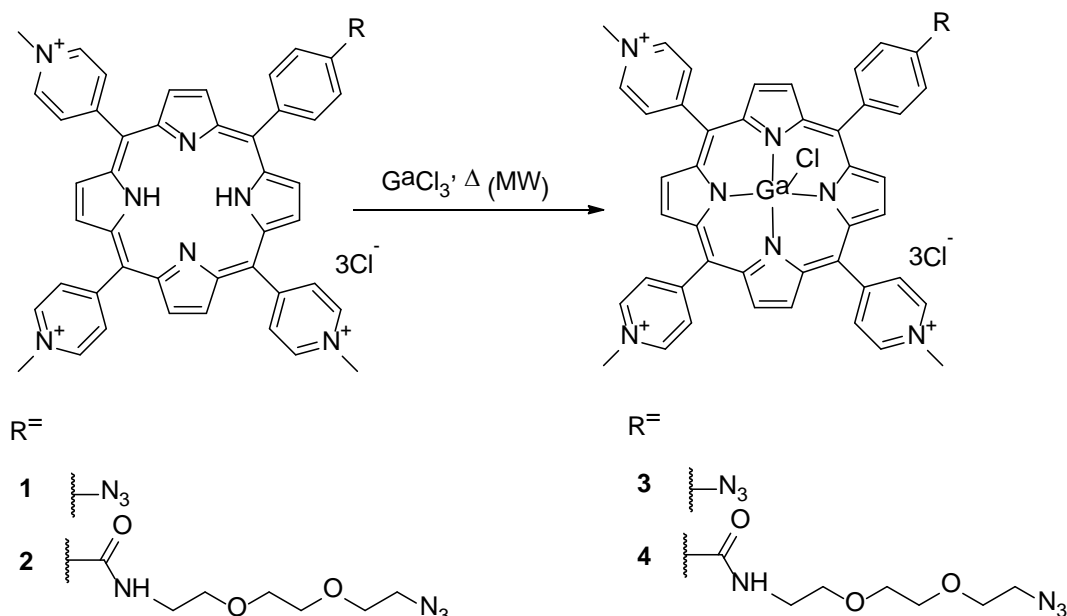


Synthesis of $^{69/71}\text{Ga}$ porphyrins

Two water-soluble cationic porphyrins bearing azide functionalities were selected for synthesis in this work. These porphyrins have previously been shown to exhibit potent cytotoxic action even when metallated with zinc,¹⁸ and also undergo click reactions rapidly without the need for reaction intensification¹⁷, important for the rapid click conjugation of a thermally-sensitive peptide following radiolabelling. Synthesis of the porphyrins was carried out according to a previously described method¹⁷, with the free base porphyrins obtained in excellent overall yield. Metallation with “cold” $^{69/71}\text{Ga}$ was then carried out to produce the gallium complex for use as HPLC standard and for use in biological evaluation (figure 2).

In previously described literature synthesis of gallium porphyrins¹⁰, microwave irradiation has been utilised in order to facilitate metal chelation, showing considerably improved rates of reaction and yields in comparison to conventional heating. Microwave irradiation also allows for solvents to be heated under pressure above their boiling points, allowing the use of water as a solvent at temperatures above 100°C. Initially, microwave heating of porphyrin **1** to 160 °C in aqueous conditions with gallium (III) chloride was shown to be extremely effective, with complete metallation observed by TLC after 1.5 minutes. However, formation of a second metallated porphyrin by-product was also observed as a result of thermal degradation of the azide functionality.

Figure 2: General metallation methodology for gallium insertion into the porphyrins.



Optimisation of reaction time and temperature demonstrated complete cessation of thermal azide degradation below 100°C, however metallation below this temperature was also slow, taking in excess of 40 minutes to achieve complete conversion to product **3**. For this reason, a reaction temperature of 110°C was selected; while some degradation was observed at this temperature with reaction times longer than 15 minutes, TLC monitoring of the reaction displayed complete conversion of the starting material to **3** after 7 minutes heating, with no appreciable formation of by-products. These optimised reaction conditions were also utilised to produce **4**; in both cases the desired product was obtained in near-quantitative yield following the described workup, with no further purification required.

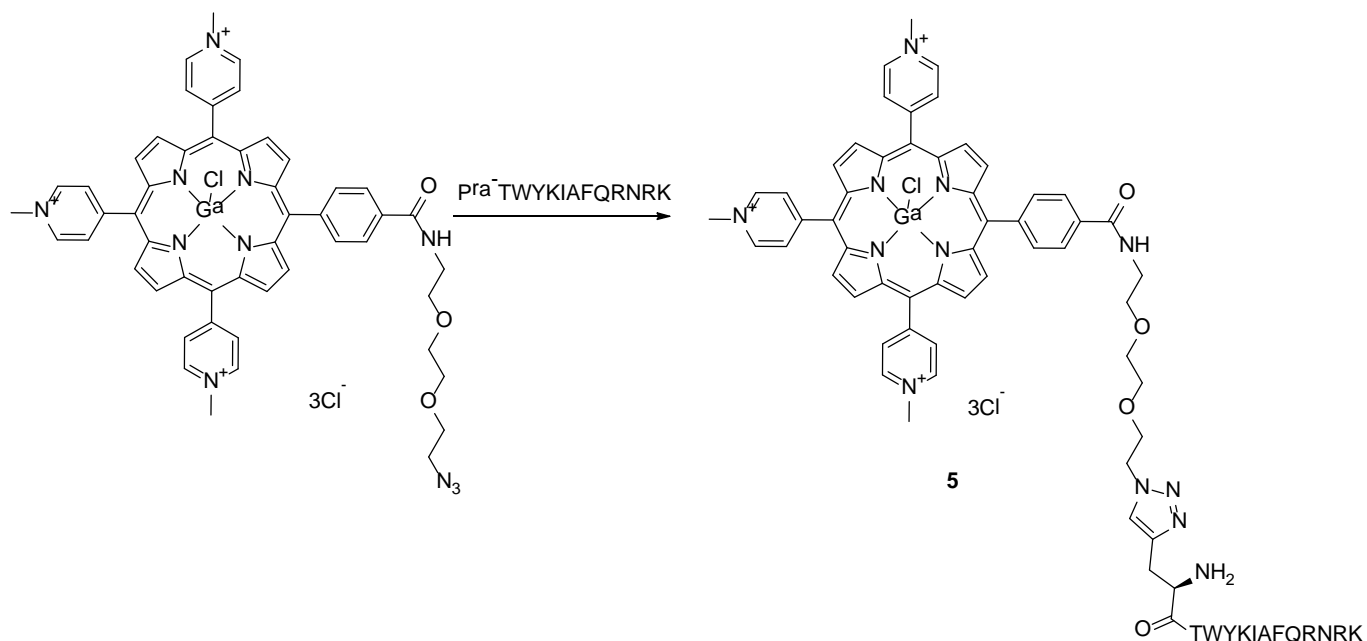
Click conjugation of $^{69/71}\text{Ga}$ porphyrin to peptide

Following the successful metallation of porphyrins **3** and **4**, click conjugation to the alkyne dodecapeptide was then attempted (figure 3). Click conjugation to the porphyrin prior to gallium insertion was not attempted as the high temperatures required for metallation are incompatible with the peptide. In addition, click conjugation prior to metallation would necessitate the inclusion of a protective metallation step to protect the porphyrin central cavity from copper insertion during the click reaction. Reaction of both porphyrins **3** and **4** with the peptide was attempted in an aqueous system at room temperature, with the reaction monitored by HPLC. Despite the similarity between the two structures, reaction rates were markedly different, with porphyrin **3** demonstrating no appreciable formation of the bioconjugate after 3 hours.

This poor reactivity was attributed to the high steric hindrance of the system, with the addition of the linker chain in porphyrin **4** significantly increasing the rate of reaction. Product formation was evident after 20 minutes reaction time, with no further reaction observed after 1 hour. Interestingly, this reaction rate is considerably slower than that observed in previous examples of the click conjugation of this porphyrin¹⁷, with the longer reaction time attributed both to the increased steric bulk of the peptide..

A one-pot, two-step metallation and click methodology was also investigated, and while neutralisation of the solution was required before addition of the peptide, no other workup was required between steps and no effect on yield or reaction time was observed. Following reaction completion, the product was purified on a Sephadex G15 column to remove unreacted starting materials and reagents, and the product lyophilised overnight to produce the desired product as characterised by HPLC and MS.

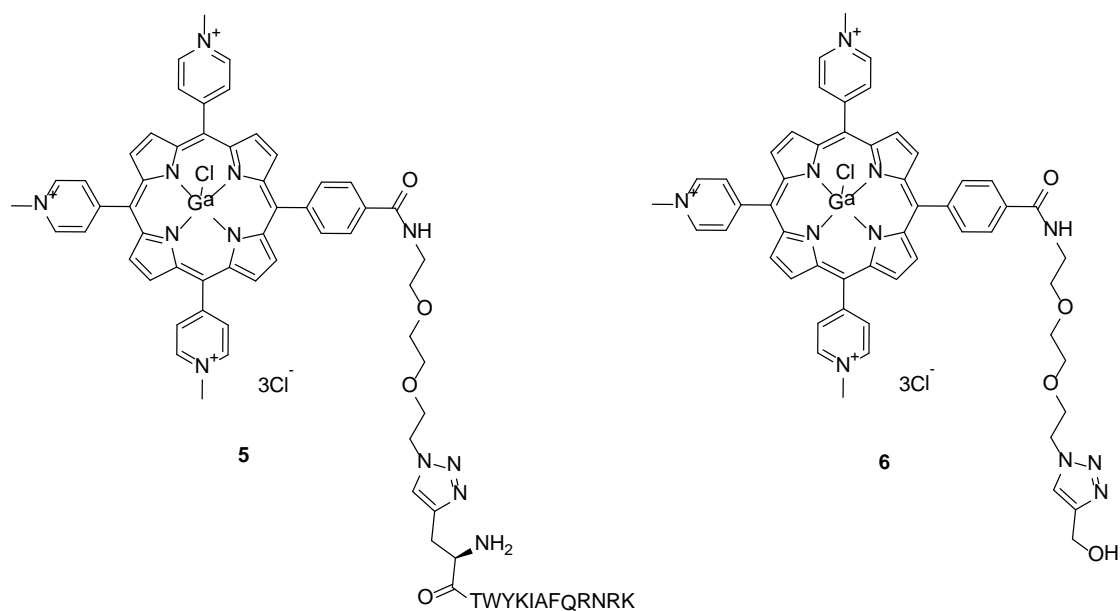
Figure 3: Click conjugation of Ga-porphyrin 4 to integrin-targeting dodecapeptide TWYKIAFQRNRK. The reaction was conducted utilising copper (II) sulfate and sodium ascorbate to generate the Cu (I) catalyst *in situ*, with addition of THPTA as a water soluble Cu (I) ligand and aminoguanidine as a sacrificial agent to protect reactive residues from side reaction with oxidised sodium ascorbate species.²⁷



Evaluation of phototoxicity

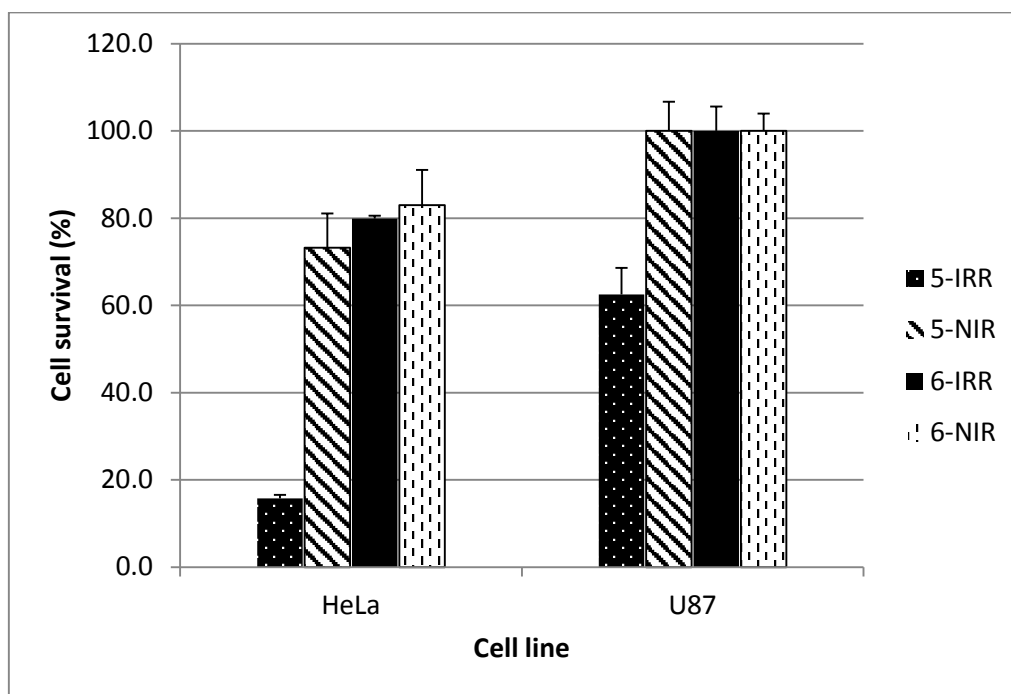
Confirmation of the potential of the targeted theranostic to differentiate between high and low integrin expressing cells was carried out through evaluation of the phototoxicity of conjugate **5** in both a highly integrin expressing cell line (HeLa) and a cell line displaying minimal integrin expression (U87). In order to confirm that the selectivity of this conjugate was as a result of the peptide targeting, synthesis of a control, untargeted porphyrin **6** was carried out through the end-capping of porphyrin **4** with propargyl alcohol to prevent potential singlet oxygen quenching by the azide functionality (figure 4). The phototoxic action of this control conjugate was then assessed in the same cell lines.

Figure 4: Structures of peptide-targeted conjugate **5** and the control, untargeted porphyrin **6**.



Irradiation of both conjugates **5** and **6** was carried out using a light system filtered to remove light below 515nm, and the results compared to a non-irradiated control. The irradiating light chosen aligns well with the position of the two Q-bands in the gallium porphyrin spectra allowing good light absorption, however excludes absorption at the porphyrin Soret band, allowing greater applicability of the results to an *in vivo* clinical setting. Under these conditions it can be seen that conjugate **5** exhibited excellent ability to eradicate the highly integrin expressing HeLa cell line (*ca.* 80% kill), while at the same concentration showing considerably lower cell killing in the U87 control cell line (Figure 5). Minimal dark toxicity was observed for this conjugate, with both cell lines displaying >75% cell survival at all concentrations in the absence of irradiation. In contrast, at the same concentrations the control porphyrin **6** displayed minimal cytotoxicity in both cell lines, with less than 20% cell kill observed in both irradiated and non-irradiated conditions for both cell lines. The limited cytotoxicity of **6** was attributed to the lack of cellular uptake; while the cellular targeting and subsequent internalisation of the $\alpha_6\beta_1$ -integrin allows uptake of conjugate **5** into target cells, no uptake of the untargeted control **6** was detected by fluorescence microscopy.

Figure 5: Graph of cytotoxicity assay. Assay was carried out on both positive (HeLa) and negative (U87) cell lines, with results displayed for conjugate **5** and control compound **6** following irradiation (IRR) and non-irradiated (NIR).



Synthesis of ^{68}Ga radiolabelled conjugate

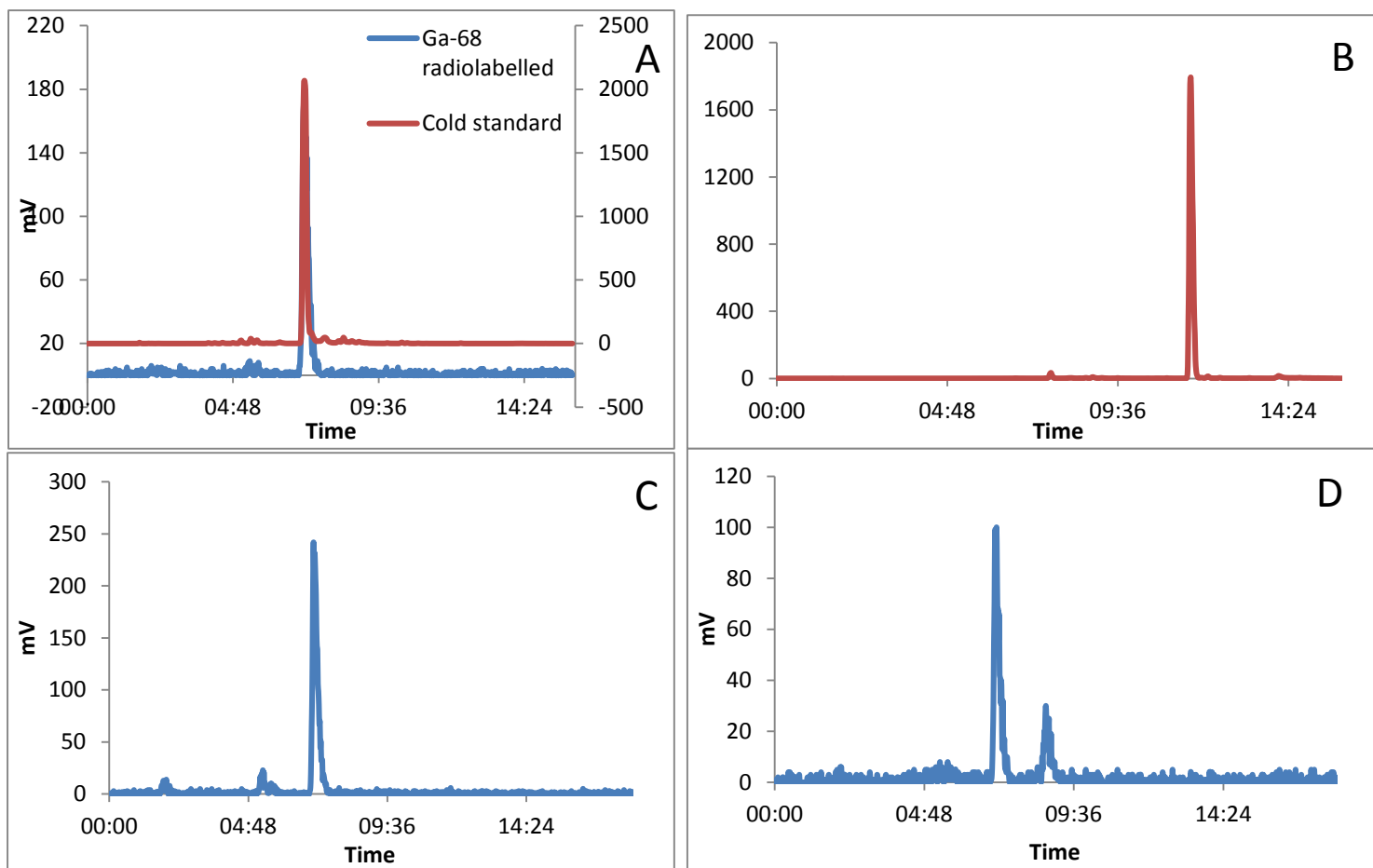
Following the successful synthesis of the $^{69/71}\text{Ga}$ conjugate **5**, development of a methodology utilising “hot” ^{68}Ga was carried out. Radiolabelling of porphyrin **2** was carried out under microwave irradiation at 110 °C due to the thermal instability of the azide functionality above this temperature. The radiolabelling was found to proceed well in 0.6M HCl at this temperature, removing the need to alter the pH or buffer the solution of ^{68}Ga prior to chelation. Increasing reaction time was not found to significantly improve radiolabelling, with reaction times of longer than five minutes showing increased formation of unlabelled by-products with little improvement in RCY, however reaction optimisation demonstrated improving radiochemical yields (RCY) with increasing quantities of porphyrin **2**, with >95% RCY obtained with addition of 20 mg of the chelating porphyrin (figure 6).

Following radiolabelling, the remaining unlabelled porphyrin was metallated with $^{69/71}\text{Ga}$ to create a carrier-added radiotracer. While the generation of such carrier-added systems is generally not optimal for PET imaging, it was preferred in this instance due to the large difference in the quantity of administered theranostic required for PET and PDT; while PET imaging is sensitive to low nanomolar quantities of radiotracers, PDT requires high nanomolar to micromolar quantities of the photosensitiser.

Administration of the carrier-added radiotracer in this way allows treatment following imaging without the need for administration of a second dose of the theranostic.

$^{69/71}\text{Ga}$ metallation was carried out under microwave heating as for the synthesis of porphyrin **4**. HPLC analysis showed that addition of the GaCl_3 directly to the solution of radiolabelled porphyrin **4-Ga68** gave poor yields, with the radiochromatogram showing formation of significant quantities of the thermal degradation by-product. Dilution of the mixture with 200 μl of water before addition of gallium (III) chloride improved solubilisation of the porphyrin in the solution, and produced essentially quantitative complexation of all unlabelled porphyrin after 3 minutes of heating with less than 10% of the thermal degradation product observed. Heating beyond this time also increased degradation of the azide and did not improve yields.

Figure 6: HPLC analysis of radiolabelling results. A: radiochromatogram of gallium-radiolabelled porphyrin **4-Ga68** overlaid with UV-chromatogram of cold standard **4**. B: UV-chromatogram of free-base porphyrin **2**. C: radiochromatogram of gallium-radiolabelled porphyrin **4-Ga68** (carrier added). D: radiochromatogram of click reaction between dodecapeptide and porphyrin **4-Ga68** to produce conjugate **5-Ga68**.



Click conjugation of the peptide to the radiolabelled porphyrin was then attempted utilising the one-pot methodology previously developed on porphyrin **4**. In this case, the dodecapeptide and the Cu (I) catalyst system were added to the radiolabelled porphyrin solution following neutralisation with sodium hydrogen carbonate, and the mixture stirred at room temperature. RadioHPLC analysis was carried to ascertain reaction completion, with the formation of the conjugate confirmed with a new peak at 8:40 minutes. A RCY of 19% was obtained after 20 minutes, with no formation of radiolabelled by-products observed. Although residual precursor porphyrin **4-Ga68** was also evident, the large difference in R_f values observed between the porphyrin **4-Ga68** and conjugate **5-Ga68** would allow for the development of a prep-HPLC methodology to isolate the pure conjugate. Alternatively, purification by Sephadex G15 as demonstrated on $^{69/71}\text{Ga}$ conjugate **5** would allow for facile isolation of the pure theranostic conjugate without the need for HPLC purification.

Conclusions

In conclusion, we have demonstrated the gallium complexation and peptide bioconjugation of an azide-functionalised porphyrin to produce a novel targeted theranostic conjugate. $\alpha_6\beta_1$ -integrin expression of three cell lines was evaluated by flow cytometry, with the FITC-labelled TWYKIAFQRNRK peptide showing good localisation in an $\alpha_6\beta_1$ -integrin overexpressing cell line. Subsequent evaluation of the therapeutic effects of the porphyrin-peptide theranostic conjugate in comparison to an untargeted control *in vitro* demonstrated good selectivity for a highly integrin expressing cell line over the control cell line, with little dark toxicity observed in both cell lines.

Experimental

Materials and methods

^1H and ^{13}C NMR spectra were recorded on JEOL Eclipse 400 and JEOL Lambda 400 spectrometers (operating at 400 MHz for ^1H and 100 MHz for ^{13}C). Chemical shifts (δ) are reported in parts per million (ppm), referenced to DMSO. Coupling constants (J) are recorded in Hz and significant multiplicities described by singlet (s), doublet (d), multiplet (m). MALDI mass spectra were performed by the EPSRC National Mass Spectrometry Facilities, Swansea, UK. UV-visible spectra were recorded on a Varian Cary spectrophotometer. Chemical reagents and solvents were purchased from Sigma-Aldrich and Alfa Aesar, and were used as received unless otherwise stated. Peptide was purchased from PeptideSynthetics. Gel filtrations were performed on Sephadex[®] G-15 medium (GE Healthcare, UK), using deionised water as the eluent. ^{68}Ga was produced on a 68Ge/68Ga iThemba LABs gallium generator, and eluted with 3 ml 0.6M HCl. Activity was measured using a Capintec Inc CRC-55t dose calibrator. Microwave reactions were carried out in a CEM Discover Benchmate microwave reactor controlled using Synergy software. In all cases, maximum stirring, maximum pressure of 200 bar and 2 minute maximum heating step were used. Reaction temperatures were monitored using an external IR probe and carried out in a 10ml sealed reaction vessel. Irradiation of cells during phototoxicity assays was carried out using an Oriel lamp system with a Schott 06515 Long Pass Optical Filter, allowing irradiation with 95-98% of light above 515 nm. RP-HPLC analyses were performed on a Agilent 1100 with a Lablogic NaI gamma detector. The separations were performed on a Gemini C1 8 column, 5 μ , 150 x 4.6 mm, 110 Å (Phenomenex, UK) at a flow rate of 1 mL/min, with a mobile phase consisting of 0.1% TFA in water (solvent A) and 0.1% TFA in acetonitrile (solvent B). Gradient: 0.0–12.0 min 0–40% solvent B, 10.2–13.9 min 95% solvent B, 13.9–14.0 min at 95–5% solvent B, 14.0–16.0 min 5% solvent B. 5-(4-azidophenyl)-10,15,20-tris(4-methylpyridiniumyl)porphyrinato trichloride, and 5-[4-2-(2-(2-azidoethoxy)ethoxy)ethanaminocarbonyl]phenyl]-10,15,20-tris(1-methyl-pyridinium-4-yl)porphyrin trichloride, were synthesised following procedures reported in the literature.¹⁸

Synthetic procedures

General procedure for synthesis of gallium porphyrins:

To a microwave tube was added the porphyrin (0.012 mmol) and water (5 ml). Gallium (III) chloride (10 mg, 0.06 mmol) was added and the mixture heated to 110°C (100W, MW) for 5 minutes. The mixture was neutralised with saturated sodium bicarbonate, and ammonium hexafluorophosphate added. The precipitated product was collected by filtration and redissolved in acetone. Tetrabutylammonium chloride was added and the precipitated product was collected by filtration. The product was precipitated from diethyl ether over methanol to yield the product as a red-purple solid.

General click reaction conditions:

To a stirred solution of gallium porphyrin (2.0 μmol) in water (1 ml) was added THPTA (174 μg , 0.4 μmol), aminoguanidine bicarbonate (54 μg , 0.4 μmol) and copper (II) sulfate pentahydrate (50 μg , 0.2 μmol) and sodium ascorbate (80 μg , 0.4 μmol) in water (0.2 ml). The dodecapeptide (2 mg, 1.7 μmol) in water (2 ml) was added and the mixture stirred at rt for 1 hour. The crude was purified on a column of Sephadex G-15, and lyophilised to remove water, to isolate the product as a pale green powder.

Cytotoxicity assays:

The Gallium-porphyrin control dye was formulated in 5%DMSO/MEM and further diluted in MEM medium (+2mM L-glutamine but no FCS) to give a range of concentrations (between 1×10^{-4} to $7.5 \times 10^{-6}\text{M}$). The Gallium-porphyrin-peptide dye was formulated in 5% DMSO/H₂O and further diluted as above to give a range of concentrations (between 3×10^{-5} to $3.75 \times 10^{-6}\text{M}$). The two cell types (HeLa and U87) were adjusted to a concentration of 1×10^6 cells/ml, added to the dilutions and incubated in the dark for an hour at 37°C and 5% CO₂ after which they were washed in a 3x excess of medium to eliminate any unbound dye. The pellets of cells and porphyrin were re-suspended in 1ml medium and 4x100 μl of each concentration put in two 96 wells plates. One plate

was irradiated with light (5.0 J/cm²) while the other served as dark toxicity control. After irradiation, 5 µl of Fetal Bovine Serum was added to each well and the plates were returned to the incubator overnight. After 18 to 24 hours, an MTT cell viability assay was performed and the results expressed as % of cell viability versus porphyrin concentration.

Flow Cytometry

Expression of α_6 -integrin on the cells, U87MG and Hela (purchased from ECAC and maintained in DMEM as described above) was assessed and quantified using flow cytometry. Cells were harvested using PBS/EDTA (12mM EDTA) and incubated with Phycoerythrin (PE) conjugated antibodies for α_6 -integrin (BD Biosciences) in DMEM supplemented with 1% BSA for 1 hour with gentle rocking at 4°C. Following labelling, cells were washed 3 times with DMEM containing 1% BSA and fixed with 1% paraformaldehyde for 15 min at 4°C. After three washes with PBS supplemented with 1% BSA, fluorescence was quantified using BD FACSCalibur. Receptor expression was quantified using calibration to fluorescence intensity using BD QuantiBRITE PE bead kit. A sample of PE labelled beads was run immediately following the experimental samples, using the same instrument settings. According to the manufacturer specification a standard curve for the fluorescence intensity and number of fluorophores per bead was constructed and used to calculate the number of receptors per cell assuming a one to one binding ratio (one PE-antibody per cellular integrin).

Radiochemistry

Labelling with gallium-68: To a microwave tube containing porphyrin 1 (20 mg, mmol) or 2 (20 mg, mmol) was added a solution of 0.6 M HCl (200 µl) containing the Ga-68 activity (10 MBq), and the solution diluted with 300 µl water. The mixture was heated to 110 °C for the required length of time (100 W, MW), and labelling yields were determined by HPLC.

Metallation with cold carrier gallium:

To a microwave tube containing the labelled porphyrin (10 MBq) in solution was added gallium (III) chloride (2 mg, 0.0012 mmol). The mixture was heated to 110 °C for the required length of time (100 W, MW), and gallium incorporation was determined by TLC (1:1:8 sat KNO₃ solution:water:acetonitrile).

Conjugation to peptide:

To a stirred solution of gallium porphyrin (1 MBq) in water (1 ml) was added THPTA (174 µg, 0.4 µmol), aminoguanidine bicarbonate (54 µg, 0.4 µmol) and copper (II) sulfate pentahydrate (50 µg, 0.2 µmol) and sodium ascorbate (80 µg, 0.4 µmol) in water (0.2 ml). The dodecapeptide (2 mg, 1.7 µmol) in water (2 ml) was added and the mixture stirred at RT for 20 mins. Radiochemical yields were determined by HPLC.

Notes and references

^a Department of Chemistry, University of Hull, Cottingham Road, HU6 7RX

^b Department of Biological Sciences, University of Hull, Cottingham Road, HU6 7RX

Mass spectrometry data was acquired at the EPSRC UK National Mass Spectrometry Facility at Swansea University.

Electronic Supplementary Information (ESI) available: synthesis and characterisation details of compounds **3-5**. See DOI: 10.1039/b000000x/

1. J. Xie, S. Lee and X. Chen, *Adv Drug Deliver Rev*, 2010, **62**, 1064-1079.
2. M. Ethirajan, Y. Chen, P. Joshi and R. K. Pandey, *Chem Soc Rev*, 2011, **40**, 340-362.
3. A. E. O'Connor, W. M. Gallagher and A. T. Byrne, *Photochem Photobiol*, 2009, **85**, 1053-1074.
4. G. A. Wagnieres, W. M. Star and B. C. Wilson, *Photochem Photobiol*, 1998, **68**, 603-632.
5. L. B. Josefsen and R. W. Boyle, *Theranostics*, 2012, **2**, 916-966.
6. J. Y. Shi, T. W. B. Liu, J. Chen, D. Green, D. Jaffray, B. C. Wilson, F. Wang and G. Zheng, *Theranostics*, 2011, **1**, 363-370.
7. H. Mukai, Y. Wada and Y. Watanabe, *Ann Nucl Med*, 2013, **27**, 625-639.
8. R. Bases, S. S. Brodie and S. Rubinfeld, *Cancer*, 1958, **11**, 259-263.
9. B. Behnam Azad, C.-F. Cho, J. D. Lewis and L. G. Luyt, *Appl Radiat Isotopes*, 2012, **70**, 505-511.
10. F. Zoller, P. J. Riss, F.-P. Montforts, D. K. Kelleher, E. Eppard and F. Rösch, *Nucl Med Biol*, 2013, **40**, 280-288.
11. Y. Fazaeli, A. Jalilian, M. Amini, K. Ardaneh, A. Rahiminejad, F. Bolourinovin, S. Moradkhani and A. Majdabadi, *Nucl Med Mol Imaging*, 2012, **46**, 20-26.
12. M. Aboudzadeh, Y. Fazaeli, H. Khodaverdi and H. Afarideh, *J Radioanal Nucl Chem*, 2013, **295**, 105-113.
13. P. A. Waghorn, *J Labelled Compd Rad*, 2014, **57**, 304-309.

14. P. Hambright, R. Fawwaz, P. Valk, J. McRae and A. J. Bearden, *Bioinorg Chem*, 1975, **5**, 87-92.
15. P. Hambright, J. C. Smart, J. McRae, M. L. Nohr, Y. Yano, P. Chu and A. J. Bearden, *Inorg Nucl Chem Lett*, 1976, **12**, 217-222.
16. F. Bryden and R. W. Boyle, *Synlett*, 2013, **24**, 1978-1982.
17. F. Giuntini, F. Bryden, R. Daly, E. M. Scanlan and R. W. Boyle, *Org Biomol Chem*, 2014, **12**, 1203-1206.
18. F. Bryden, A. Maruani, H. Savoie, V. Chudasama, M. E. B. Smith, S. Caddick and R. W. Boyle, *Bioconjugate Chem*, 2014, **25**, 611-617.
19. V. V. Rostovtsev, L. G. Green, V. V. Fokin and K. B. Sharpless, *Angew Chem Int Ed*, 2002, **41**, 2596-2599.
20. M. Fathalla, S.-C. Li, U. Diebold, A. Alb and J. Jayawickramarajah, *Chem Commun*, 2009, **0**, 4209-4211.
21. M. T. Ma, O. C. Neels, D. Denoyer, P. Roselt, J. A. Karas, D. B. Scanlon, J. M. White, R. J. Hicks and P. S. Donnelly, *Bioconjugate Chem*, 2011, **22**, 2093-2103.
22. R. Haubner, S. Maschauer and O. Prante, *BioMed Research International*, 2014, **2014**, 17.
23. H. Nakahara, M. Nomizu, S. K. Akiyama, Y. Yamada, Y. Yeh and W.-T. Chen, *J Biol Chem*, 1996, **271**, 27221-27224.
24. E. V. Rosca, R. J. Gillies and M. R. Caplan, *Biotechnology and Bioengineering*, 2009, **104**, 408-417.
25. U. M. Wewer, L. M. Shaw, R. Albrechtsen and A. M. Mercurio, *Am. J. Pathol.*, 1997, **151**, 1191-1198.
26. E. V. Rosca, J. M. Stukel, R. J. Gillies, J. Vagner and M. R. Caplan, *Biomacromolecules*, 2007, **8**, 3830-3835.
27. S. I. Presolski, V. P. Hong and M. G. Finn, in *Current Protocols in Chemical Biology*, John Wiley & Sons, Inc., 2009.